

See discussions, stats, and author profiles for this publication at: <https://www.researchgate.net/publication/231232607>

Fabrication and Properties of Eight Novel Lanthanide–Organic Frameworks Based on 4-Hydroxypyran-2,6-dicarboxylate and 4-Hydroxypyridine-2,6-dicarboxylate

ARTICLE *in* CRYSTAL GROWTH & DESIGN · SEPTEMBER 2009

Impact Factor: 4.89 · DOI: 10.1021/cg900146y

CITATIONS

21

READS

16

6 AUTHORS, INCLUDING:



Bin Zhao

Nankai University

126 PUBLICATIONS 5,391 CITATIONS

SEE PROFILE

Fabrication and Properties of Eight Novel Lanthanide–Organic Frameworks Based on 4-Hydroxypyran-2,6-dicarboxylate and 4-Hydroxypyridine-2,6-dicarboxylate

Ming Fang, Lixian Chang, Xuhui Liu, Bin Zhao,* Ya Zuo, and Zhi Chen

Department of Chemistry, Nankai University, Tianjin 300071, P. R. China

Received February 8, 2009; Revised Manuscript Received June 19, 2009

ABSTRACT: Eight novel lanthanide–organic frameworks, $[\text{Ln}(\text{CDA})]$ ($\text{Ln} = \text{Pr}$ (**1**), Nd (**2**), Sm (**3**), $\text{CDA} = 4\text{-hydroxypyran-2,6-dicarboxylate}$), $[\text{Ho}(\text{CDA})(\text{H}_2\text{O})]$ (**4**), $[\text{Pr}(\text{HCDA})(\text{C}_2\text{O}_4)_{0.5}(\text{H}_2\text{O})_2]$ (**5**), $[\text{Lu}(\text{CDA})\text{Ba}_2(\text{C}_2\text{O}_4)_2(\text{H}_2\text{O})_2] \cdot 0.25\text{CH}_3\text{OH}$ (**6**), $[\text{Dy}(\text{HCAM})_2(\text{CAM})\text{Ba}_2(\text{H}_2\text{O})_{9.75}] \cdot 7.625\text{H}_2\text{O}$ (**7**), $\text{CAM} = 4\text{-hydroxypyridine-2,6-dicarboxylate}$), $[\text{Sm}_2(\text{CAM})_4\text{Ba}_3(\text{H}_2\text{O})_2]$ (**8**), have been synthesized under hydrothermal conditions. They were structurally characterized by single-crystal X-ray diffraction. Compounds **1–3** are isostructural and display novel three-dimensional (3D) architectures, and compound **4** features a two-dimensional (2D) double-layer structure. The structural divergence between **1–3** and **4** may originate from a lanthanide contraction effect. By increasing the temperature during the synthesis of **1**, CDA was partly decomposed into oxalate ions, and as a result, compound **5** with a 3D framework different from that of **1** was obtained. The Lu-based compound isostructural to **4** has not been obtained so far under synthetic conditions similar to that of **1–4**. However, by replacing LiOH with $\text{Ba}(\text{OH})_2$, heterometallic $[\text{LuBa}]$ compound **6** was successfully synthesized, exhibiting a 3D framework. After changing CDA into CAM based on the synthesis of **6**, compounds **7** with a one-dimensional (1D) chain and **8** with a sandwich-like 3D structure were produced. Luminescence analyses were performed on compounds **7** and **8**, which exhibit the characteristic transitions of corresponding lanthanide ions. The magnetic susceptibilities of **5** and **7** were measured and discussed.

Introduction

The crystal engineering of metal–organic frameworks (MOFs) is becoming an increasingly popular field of research in view of the potential applications and unusual topologies of these new materials.^{1–3} And many spectacular MOFs have been obtained.⁴ However, in contrast to the numerous transition metal–organic frameworks, the design and control over lanthanide-based frameworks is a difficult task because of their high and variable coordination number and flexible coordination environment. On the other hand, lanthanide ions with the specific character mentioned above are good candidates to provide unique opportunities for the discovery of intriguing MOFs. Actually, it is well-known that organic ligands play rather important roles in the construction of MOFs, and multicarboxylate ligands are frequently chosen because of their rich coordination modes. In this contribution, 4-hydroxypyran-2,6-dicarboxylate (CDA)⁵ was selected to fabricate lanthanide–organic frameworks according to the following advantages: (a) higher symmetry of the ligand may cause the generations of ordered structures; (b) the rigidity of the ligand may reduce the possibility of lattice interpenetration in products; (c) the multidentate carboxylate is known to be essential in chelating lanthanide ions to form chain-like units with $\text{Ln}–\text{O}–\text{Ln}$ connectivity; (d) this ligand contains two carboxylic groups, and two other oxygen atoms, so it may chelate to metal ions as a multidentate ligand and by using various coordination modes to form fascinating multidimensional compounds. 4-Hydroxy-pyridine-2,6-dicarboxylate (CAM)⁶ has a structure similar to the CDA ligand; we were interested in whether a similar ligand structure would produce a similar coordination polymer.

We know that reaction conditions, for example, the reaction temperature and the amount and the kind of alkali, have a great influence during the fabrication of lanthanide-based MOFs, thus leading us to this interesting and challenging field. It is worth noting that MOFs associated with both lanthanide ions and barium ions received less regard. Because of the big atom radius of barium ion, it displays variable coordination modes, which may lead to a fancier structure.

In this contribution, eight novel compounds with various topological structures: $[\text{Ln}(\text{CDA})]$ ($\text{Ln} = \text{Pr}$ (**1**), Nd (**2**), Sm (**3**), $\text{CDA} = 4\text{-hydroxypyran-2,6-dicarboxylate}$), $[\text{Ho}(\text{CDA})(\text{H}_2\text{O})]$ (**4**), $[\text{Pr}(\text{HCDA})(\text{C}_2\text{O}_4)_{0.5}(\text{H}_2\text{O})_2]$ (**5**), $[\text{Lu}(\text{CDA})\text{Ba}_2(\text{C}_2\text{O}_4)_2(\text{H}_2\text{O})_2] \cdot 0.25\text{CH}_3\text{OH}$ (**6**), $[\text{Dy}(\text{HCAM})_2(\text{CAM})\text{Ba}_2(\text{H}_2\text{O})_{9.75}] \cdot 7.625\text{H}_2\text{O}$ (**7**), $\text{CAM} = 4\text{-hydroxypyridine-2,6-dicarboxylate}$), $[\text{Sm}_2(\text{CAM})_4\text{Ba}_3(\text{H}_2\text{O})_2]$ (**8**), were fabricated by tuning synthetic conditions and structurally characterized from a one-dimensional (1D) chain, two-dimensional (2D) double-layer, to three-dimensional (3D) networks. Luminescence analyses were performed on compounds **7** and **8**, which exhibit the characteristic transitions of corresponding lanthanide ions.

Experimental Section

Materials and Physical Measurements. All chemicals purchased were of reagent grade and used without further purification. Water used in the reactions was distilled water. The elemental analyses (C, H, and N) were carried out a Perkin-Elmer elemental analyzer. The fluorescent spectra were measured on a Varian Cary Eclipse Fluorescence spectrophotometer.

Syntheses of **1–4.** A mixture of H_3CDA (0.162 g, 0.8 mmol), $\text{LiOH} \cdot \text{H}_2\text{O}$ (0.029 g, 0.7 mmol), 0.2 mmol of $\text{Ln}(\text{NO}_3)_3 \cdot 6\text{H}_2\text{O}$ ($\text{Ln} = \text{Pr}$ (**1**, 0.087 g); Nd (**2**, 0.088 g); Sm (**3**, 0.089 g); Ho (**4**, 0.092 g)), water (6 mL), and ethanol (4 mL) was sealed in a 25 mL stainless steel reactor with a Teflon-liner and heated at 120 °C for 3 days, then cooled to room temperature in 1 day. The crystals of **1–4** were

Table 1. Crystallographic Data and Structure Refinement Details for 1–4

	1	2	3	4
formula	C ₇ H ₂ O ₆ Pr	C ₇ H ₂ O ₆ Nd	C ₇ H ₂ O ₆ Sm	C ₇ H ₄ O ₇ Ho
M _r	323	326.33	332.44	365.03
crystal system	orthorhombic	orthorhombic	orthorhombic	orthorhombic
space group	Pnma	Pnma	Pnma	Pnma
a (Å)	7.9153(18)	7.9247(12)	7.9263(14)	19.476(5)
b (Å)	10.228(2)	10.2187(15)	10.2173(18)	10.024(3)
c (Å)	9.528(2)	9.5383(14)	9.5413(17)	4.3060(12)
α (°)	90	90	90	90
β (°)	90	90	90	90
γ (°)	90	90	90	90
V (Å ³)	771.4(3)	772.4(2)	772.7(2)	840.6(4)
Z, ρ _{calc} (Mg/m ³)	4, 2.781	4, 2.806	4, 2.858	4, 2.884
μ (mm ⁻¹)	6.314	6.720	7.589	9.426
F(000)	604	608	616	676
θ range (°)	2.92–26.42	2.92–25.02	2.92–25.01	2.09–25.02
limiting indices	−9 ≤ h ≤ 8	−9 ≤ h ≤ 9	−8 ≤ h ≤ 9	−17 ≤ h ≤ 23
	−12 ≤ k ≤ 7	−12 ≤ k ≤ 12	−12 ≤ k ≤ 11	−11 ≤ k ≤ 11
	−11 ≤ l ≤ 11	−6 ≤ l ≤ 11	−7 ≤ l ≤ 11	−5 ≤ l ≤ 5
reflns collected	4049	3648	3623	3779
GOF on F ²	1.163	1.166	1.109	1.127
R ₁ /wR ₂ [I > 2σ(I)]	R ₁ = 0.0340	R ₁ = 0.0219, wR ₂ = 0.0579	R ₁ = 0.0247	R ₁ = 0.0358 wR ₂ = 0.0961
R ₁ /wR ₂ (all data)	R ₁ = 0.0218, wR ₂ = 0.0535	R ₁ = 0.0242, wR ₂ = 0.0589	R ₁ = 0.0256, wR ₂ = 0.0630	R ₁ = 0.0404, wR ₂ = 0.1009

Table 2. Crystallographic Data and Structure Refinement Details for 5–8

	5	6	7	8
formula	C ₈ H ₇ O ₁₀ Pr	C _{11.25} H ₇ Ba ₂ LuO _{16.25}	C ₂₁ H _{42.75} Ba ₂ DyN ₃ O _{32.375}	C ₂₈ H ₁₂ Ba ₃ N ₄ O ₂₂ Sm ₂
M _r	404.05	851.82	1292.78	1469.14
crystal system	monoclinic	monoclinic	triclinic	monoclinic
space group	C2/c	P2(1)/n	P̄1	P2(1)/n
a (Å)	21.507(2)	11.1975(19)	11.484(2)	15.254(3)
b (Å)	6.8401(8)	11.4686(15)	12.500(2)	15.472(3)
c (Å)	16.2843(19)	15.8001(19)	15.790(3)	15.524(3)
α (°)	90	90	102.815(3)	90
β (°)	120.453(2)	106.3140(10)	105.458(3)	119.36(3)
γ (°)	90	90	90.378(3)	90
V (Å ³)	2065.1(4)	1947.3(5)	2125.0(6)	3193.0(11)
Z, ρ _{calc} (Mg/m ³)	8, 2.599	4, 2.905	2, 2.027	4, 3.056
μ (mm ⁻¹)	4.773	9.112	3.679	7.375
F(000)	1552	1550	1256	2704
θ range (°)	2.20–26.37	1.99–26.34	1.38–25.02	2.00–25.60
limiting indices	−22 ≤ h ≤ 26	−13 ≤ h ≤ 11	−13 ≤ h ≤ 11	−13 ≤ h ≤ 18
	−8 ≤ k ≤ 7	−14 ≤ k ≤ 11	−14 ≤ k ≤ 13	−17 ≤ k ≤ 18
	−20 ≤ l ≤ 20	−19 ≤ l ≤ 19	−18 ≤ l ≤ 18	−18 ≤ l ≤ 16
reflns collected	5603	10674	10955	17563
GOF on F ²	1.295	1.134	1.057	1.085
R ₁ /wR ₂ [I > 2σ(I)]	R ₁ = 0.0278	R ₁ = 0.0386 wR ₂ = 0.0970	R ₁ = 0.0471 wR ₂ = 0.1058	R ₁ = 0.0321 wR ₂ = 0.0620
R ₁ /wR ₂ (all data)	R ₁ = 0.0307	R ₁ = 0.0447 wR ₂ = 0.0994	R ₁ = 0.0758 wR ₂ = 0.1190	R ₁ = 0.0404 wR ₂ = 0.0656

obtained in 23%, 26%, 21%, and 28% yields (based on Ln(NO₃)₃·6H₂O), respectively. Anal. calcd. for C₇H₂O₆Pr: C, 26.03; H, 0.62. Found: C, 25.86; H, 0.49. Anal. Calcd for C₇H₂O₆Nd: C, 25.76; H, 0.61. Found: C, 25.58; H, 0.51. Anal. Calcd for C₇H₂O₆Sm: C, 25.29; H, 0.6. Found: C, 25.10; H, 0.38. Anal. calcd. for C₇H₄O₇Ho: C, 23.03; H, 1.10. Found: C, 22.87; H, 0.98.

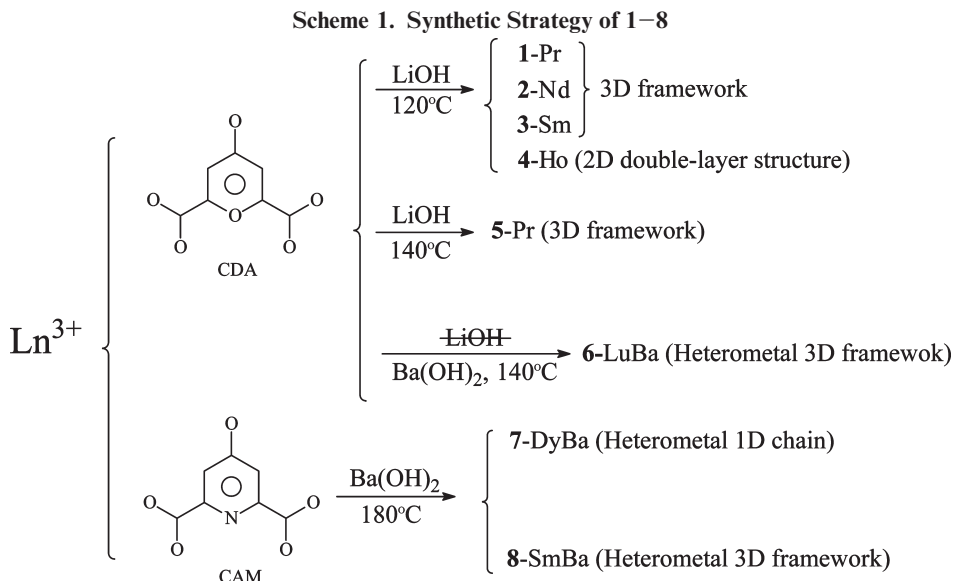
Synthesis of [Pr(HCDA)(C₂O₄)_{0.5}(H₂O)₂] (5). In a typical synthesis for **5**, a mixture of H₃CDA (0.162 g, 0.8 mmol), LiOH·H₂O (0.029 g, 0.7 mmol), Pr(NO₃)₃·6H₂O (0.087 g, 0.2 mmol), water (6 mL), and ethanol (4 mL) was sealed in a 25 mL stainless steel reactor with a Teflon-liner and heated at 140 °C for 3 days, then cooled to room temperature in 1 day. The crystals of **5** were obtained in 18% yield (based on Pr(NO₃)₃·6H₂O). Anal. calcd. for C₈H₇O₁₀Pr: C, 23.78; H, 1.74. Found: C, 23.62; H, 1.58.

Synthesis of [Lu(CDA)Ba₂(C₂O₄)₂(H₂O)₂]·0.25CH₃OH (6). In a typical synthesis for **6**, a mixture of H₃CDA (0.162 g, 0.8 mmol), Ba(OH)₂·H₂O (0.119 g, 0.63 mmol), Lu(NO₃)₃·6H₂O (0.094 g, 0.2 mmol), water (6 mL), and methanol (4 mL) was sealed in a 25 mL stainless steel reactor with a Teflon-liner and heated at 140 °C for 3 days, then cooled to room temperature in 1 day. The crystals of **6**

were obtained in 37% yield (based on Lu(NO₃)₃·6H₂O). Anal. calcd. for C_{11.50}H₇Ba₂LuO_{16.25}: C, 16.15; H, 0.83. Found: C, 16.32; H, 0.64.

Syntheses of [Dy(HCAM)₂(CAM)Ba₂(H₂O)_{9.75}]·7.625H₂O (7) and [Sm(CAM)₄Ba₃(H₂O)₂] (8). A mixture of H₃CAM (0.146 g, 0.8 mmol), Ba(OH)₂·H₂O (0.114 g, 0.6 mmol), 0.2 mmol of Ln(NO₃)₃·6H₂O (Ln=Dy (7), 0.091 g; Sm (8), 0.089 g) and water (10 mL) was sealed in a 25 mL stainless steel reactor with a Teflon-liner and heated at 180 °C for 3 days, then cooled to room temperature in 1 day. The crystals of **7** and **8** were obtained in 41% and 38% yields (based on Ln(NO₃)₃·6H₂O), respectively. Anal. Calcd for C₂₁H_{44.75}Ba₂DyN₃O_{32.375}: C, 19.48; H, 3.48; N, 3.25. Found: C, 19.32; H, 3.26; N, 3.12. Anal. Calcd for C₂₈H₁₂Ba₃N₄O₂₂: C, 22.89; H, 0.82; N, 3.81. Found: C, 22.75; H, 0.62; N, 3.65.

Crystallographic Studies. Single-crystal X-ray diffraction measurements of **1–8** were carried out with a Bruker Smart CCD diffractometer and a graphite crystal monochromator situated in the incident beam for data collection at 294(2) K. Lorentz polarization and absorption corrections were applied. The structures were solved by direct methods and refined by full-matrix least-squares



techniques using the SHELXS-97 and SHELXL-97 programs.⁷ Anisotropic thermal parameters were assigned to all non-hydrogen atoms. The hydrogen atoms were placed in idealized positions. It should be noted that the hydrogen atoms of all lattice water molecules in these complexes were not located by difference Fourier Map, and thus some A-type errors related to the case in CIF-check files may be observed, just as compound 7. Crystallographic data for **1–8** are summarized in Tables 1 and 2. Selected bond lengths and angles were summarized in Table S1 in Supporting Information.

Results and Discussion

Syntheses. The eight complexes were obtained by hydrothermal reaction and the synthetic strategy of **1–8** was shown in Scheme 1. Compounds **1–3** which are isomorphous, exhibit interesting 3D framework. Because of the influence of lanthanide contraction effect, compound **4** displays a 2D double-layer structure which is different from those of compounds **1–3**. As we changed the temperature from 120 to 140 °C during synthesizing **1** to explore the influence of temperature on structures, as a result, compound **5** with a 3D framework was obtained in which the CDA ligand was partly decomposed into oxalate. After attempt to acquire the crystals of [Lu-CDA] compound was failure by adjusting the amount of LiOH, Ba(OH)₂ was selected to instead of LiOH. Surprisingly, we got a 3D heterometal-organic framework [Ln-Ba-CDA] (**6**). Inspired by this, according to the structural similarity between CDA and CAM, the construction of heterometal-organic frameworks [Ln-Ba-CAM] was carried out by applying CAM as a ligand, and compound **7** with 1D chain structure and compound **8** with 3D architecture were produced.

Crystal Structure of [Ln(CDA)] (Ln = Pr (1**), Nd (**2**), Sm (**3**), CDA = 4-hydroxypyran-2,6-dicarboxylate).** Single crystal X-ray diffraction analysis reveals that the three compounds are isomorphous, belonging to orthorhombic system with space group *Pnma*, and therefore, the structure of compound **1** is described here in detail. There exists one crystallographically independent Pr³⁺, one CDA molecule in the asymmetric unit (Figure 1). Six carboxylic oxygen atoms of five CDA ligands and two hydroxyl oxygen atoms (O3A and O3B) from another two CDA ligand complete the coordinated sphere of Pr³⁺, and the coordination geometry for the eight-coordinated Pr³⁺ can be described as a distorted bicapped trigonal prism in which O3 act as the capping atom. The

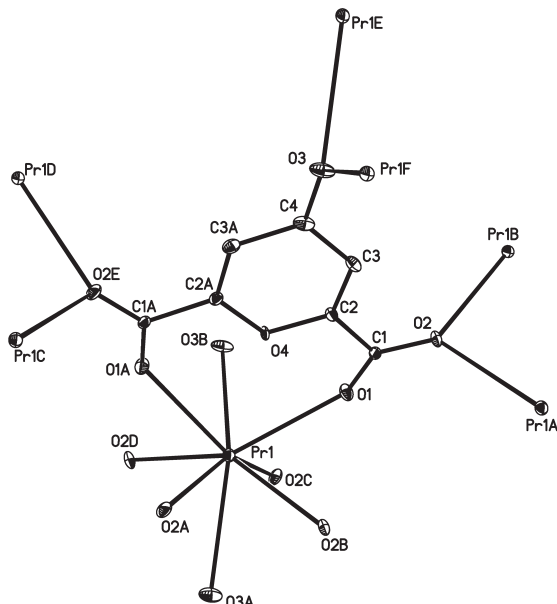


Figure 1. Molecule structure of **1**, showing the coordination environments of Pr³⁺ and CDA ligand.

Pr–O distances are in the range of 2.723(4)–2.883(4) Å. The CDA anion acts as a heptadentate metal linker (Figure 1): two carboxylic oxygen atoms of CDA chelate with one Pr³⁺ in a bidentate fashion (O1 and O1A) and the other two carboxylic oxygen atoms bridges to four Pr³⁺ (Pr1A, Pr1B, Pr1C, and Pr1D) as well as the hydroxyl oxygen atoms coordinate to two Pr³⁺ (Pr1E and Pr1F). Through the bridging of carboxylic and hydroxyl oxygen atoms, the Pr³⁺ form a 1D chain along the *a* direction, which is further connected into a 3D framework by carboxylic groups (Figure 2). Both the ligand and Pr³⁺ can be considered as a seven-connected node. Thus, the network of compound **1** can be described as an Archimedean-type net with two nonequivalent points: (4¹⁷6⁴)(4¹⁵6⁶), as shown in Figure 3.

Crystal Structure of [Ho(CDA)(H₂O)] (4**).** The X-ray structural analysis reveals that **4** is orthorhombic crystal system, space group *Pnma*. The self-assembly of H₃CDA with Ho(III) salts gave a 2D coordination polymer **4**. Four

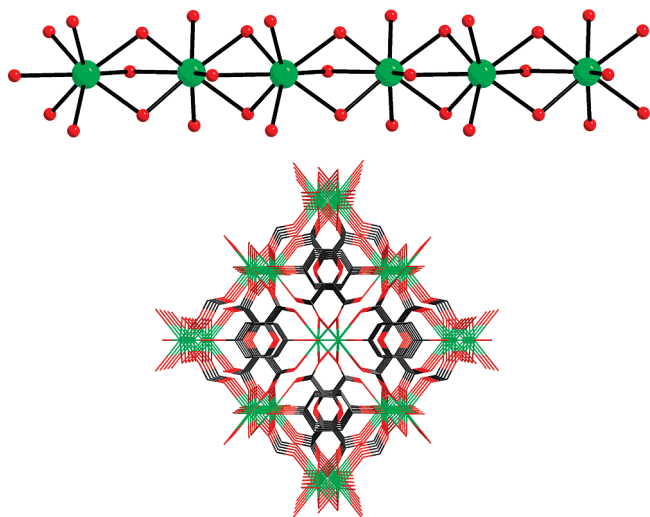


Figure 2. (top) The 1D chain structure of compound **1** viewed along the *c* direction; (bottom) the 3D framework of compound **1**. Color codes: red, O; green, Pr.

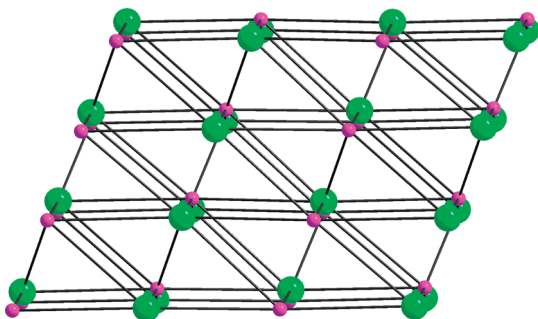


Figure 3. The topological structure of compound **1**. Color codes: green, Pr, purple, ligand.

carboxylic oxygen atoms, one hydroxyl oxygen atom and one water molecule complete the six coordinated sphere of Ho^{3+} , and the coordination geometry can be described as a distorted octahedral geometry. The CDA anion acts as a pentadentate ligand. Every carboxylic group has one oxygen atom coordinated to two Ho^{3+} , and the hydroxyl oxygen atoms coordinate to one Ho^{3+} (Figure 4). The $\text{Ho}-\text{O}$ -
(carboxylic) distances are in the range of $2.681(6)$ – $2.838(4)$ Å, $\text{Ho}-\text{O}$ (aqua) bond is $2.768(4)$ Å. Viewed along a direction, the Ho^{3+} are connected into a 1D chain through carboxylic oxygen atoms, which are further assembled into a 2D double-layer structure by the linking of the ligand, as shown in Figure 5. The 2D structure may be regarded as a (5, 5) topological network with both the ligand and Ho^{3+} acting as “five-connected” nodes, and thus **4** may be described as an Archimedean-type net with two nonequivalent points: $(4^86^2)(4^86^2)$, as shown in Figure 6.

Crystal Structure of $[\text{Pr}(\text{HCDA})(\text{C}_2\text{O}_4)_{0.5}(\text{H}_2\text{O})_2]$ (5). There is one crystallographically independent Pr^{3+} , one CDA molecule, half oxalate, and two coordinated water molecules in the asymmetric unit (Figure 7). A tridentate CDA ligand, three carboxylic oxygen atoms ($\text{O}1\text{A}$, $\text{O}4\text{B}$ and $\text{O}5\text{B}$) from two CDA ligands, two oxalate oxygen atoms ($\text{O}7$ and $\text{O}8\text{A}$), and two water molecules ($\text{O}9$ and $\text{O}10$) complete the coordinated environment of Pr^{3+} . The $\text{Pr}-\text{O}$ distances are in the range of $2.405(4)$ – $2.863(4)$ Å. Interestingly, the CDA ligand is partly decomposed into oxalate that makes the

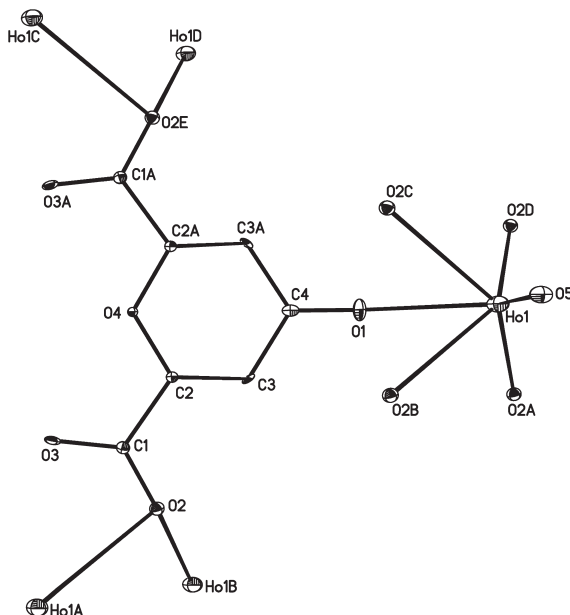


Figure 4. Molecule structure of **4**, showing the coordination environments of Ho^{3+} and CDA ligand.

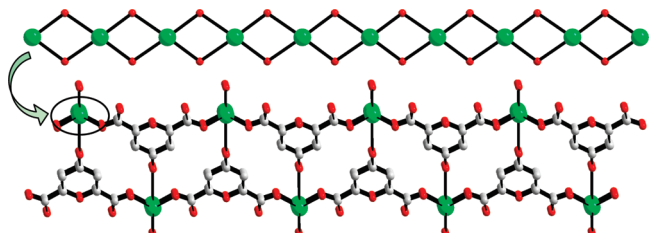


Figure 5. (top) The 1D chain view along the *a* direction of compound 4; (bottom) the 2D double-layer structure of compound 4. Color codes: red, O; gray, C; green, Ho.

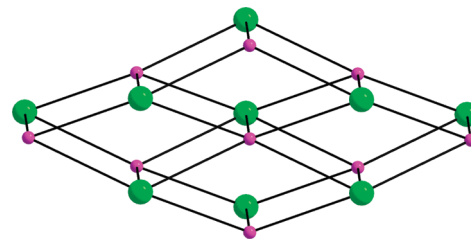


Figure 6. The topological structure of compound **4**. Color codes: green, Pr, purple, ligand.

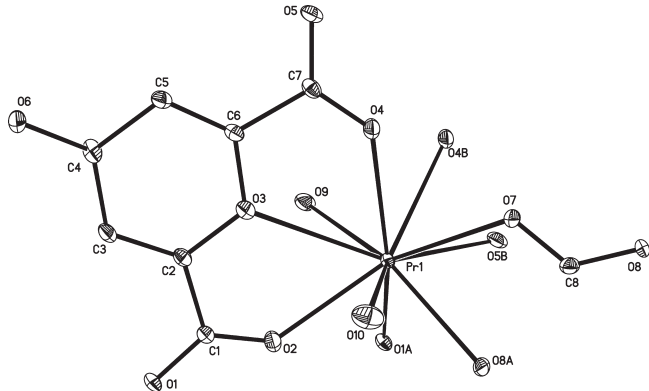


Figure 7. Molecule structure of **5**, showing the coordination environments of Pr^{3+} and CDA ligand.

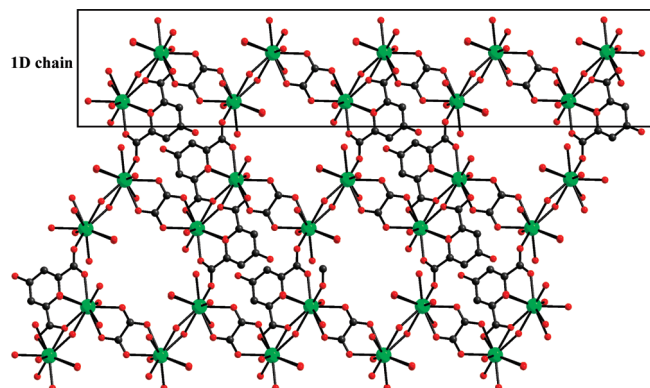


Figure 8. The 2D layer of compound **5**, including a 1D chain motif shown in the square. Color codes: red, O; black, C; green, Pr.

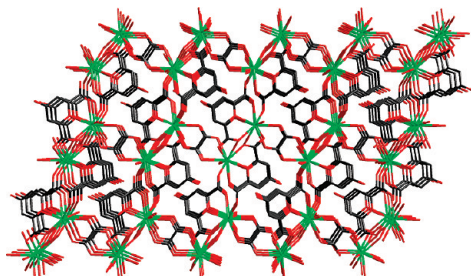


Figure 9. The 3D framework of compound **5**.

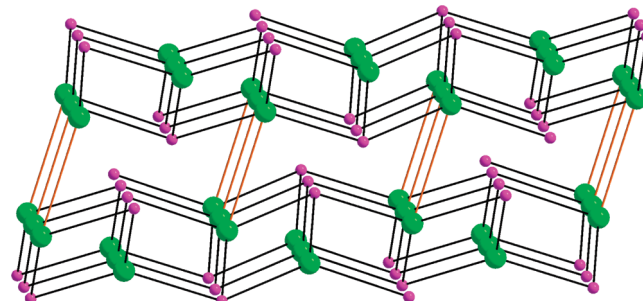


Figure 10. The topological structure of compound **5**; the oxalate was simplified as a line (yellow). Color codes: green, Pr; purple, the CDA ligand.

structure very charming. In the *ac* plane, two carboxylic oxygen atoms from two CDA ligands and the oxalate acts as a bridge, alternately linking the Pr^{3+} into a 1D zigzag chain; the 1D chain is further assembled into a 2D layer by carboxyl group bridges (Figure 8). Then the 2D layer is further connected into a 3D framework by carboxyl group bridges (Figure 9). Topologically, every Pr^{3+} connects to four CDA ligands, while every CDA ligand connects to three Pr^{3+} . Thus, Pr^{3+} and the CDA ligand can be defined as a 4- and 3-connected node, respectively. The oxalate ions that link with two Pr^{3+} can be simplified as a line. On the basis of this simplification, the structure of **5** can be described as an $(468)(46^28^210)$ topological network (Figure 10).

Crystal Structure of $[\text{Lu}(\text{CDA})\text{Ba}_2(\text{C}_2\text{O}_4)_2(\text{H}_2\text{O})_2] \cdot 0.25\text{CH}_3\text{OH}$ (6). The self-assembly of H_3CAM with $\text{Lu}(\text{III})$ salts and $\text{Ba}(\text{OH})_2$ gave a 3D coordination polymer **6**. The X-ray structural analysis reveals that **6** is monoclinic crystal system, space group $P2(1)/n$. The asymmetric unit of **6** consists of one crystallographically independent Lu^{3+} , two Ba^{2+} , one CDA ligand, two oxalate anions, two coordinated water

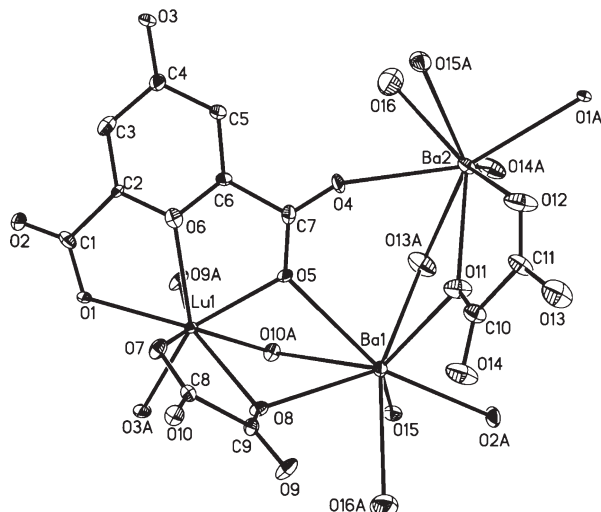


Figure 11. Molecule structure of **6**, showing the coordination environments of Lu^{3+} , Ba^{2+} , and CDA ligand.

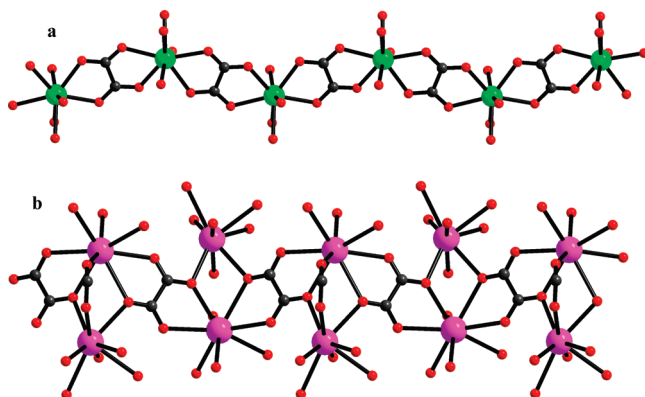


Figure 12. (a) the 1D chain structure of Lu^{3+} of compound **6** linked by oxalate anions; (b) the 1D chain of Ba^{2+} of compound **6** linked by oxalate anions. Color codes: red, O; black, C; green, Lu; purple, Ba.

molecules, and one-quarter of a methanol molecule (Figure 11). A tridentate CDA ligand, one hydroxyl oxygen atom of another CDA ligand, and four $\text{O}_{\text{C}_2\text{O}_4}$ atoms complete the coordinated environment of Lu^{3+} , which displays a distorted bicapped trigonal prism geometry. The Lu–O distances are in the range of $2.220(4)$ – $2.391(4)$ Å. There are two kinds of barium atoms: Ba1 and Ba2, and they are all eight-coordinated. The coordinated spheres of both Ba1 and Ba2 consist of two carboxylic oxygen atoms of CDA, four $\text{O}_{\text{C}_2\text{O}_4}$ atoms and two water molecules, and the corresponding coordination geometry of Ba1 and Ba2 can be described as a distorted bicapped trigonal prism. The Ba–O distances are in the range of $2.651(5)$ – $3.048(7)$ Å. One of two $\text{C}_2\text{O}_4^{2-}$ anions chelates to Ba2 in a bidentate mode (O11 and O12), and the other chelates with Lu1 by O7 and O8. Two μ_2 -O (O11 and O13A) atoms and one carboxyl group bridge Ba1 and Ba2. Lu1 and Ba1 are linked by three μ_2 -O (O5, O8 and O10A), while Lu1 and Ba2 only are bridged by one carboxyl group (O4C7O5).

Interestingly, the CDA ligand is partly decomposed into oxalate ions which display a very important role in the construction of the structure. Lu^{3+} is connected into a 1D chain along the *a* direction by the bridging of an oxalate group (Figure 12a), then the 1D chain is further connected into a 2D layer (2D-Lu-layer) by the ligands. In the 2D-Lu-layer,

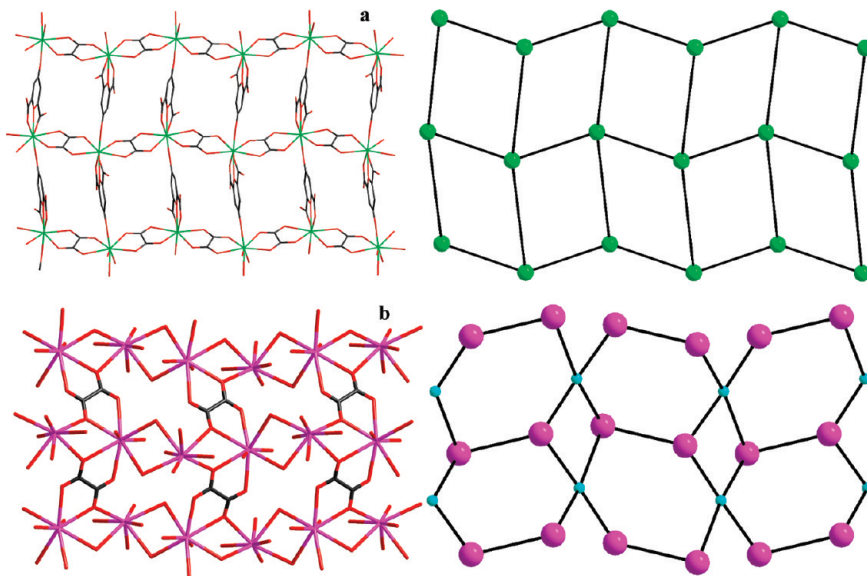


Figure 13. (a) The 2D layer of Lu^{3+} and (b) the 2D layer of Ba^{2+} in compound **6**. Color codes: red, O; black, C; green, Lu; purple, Ba; blue, oxalate ion.

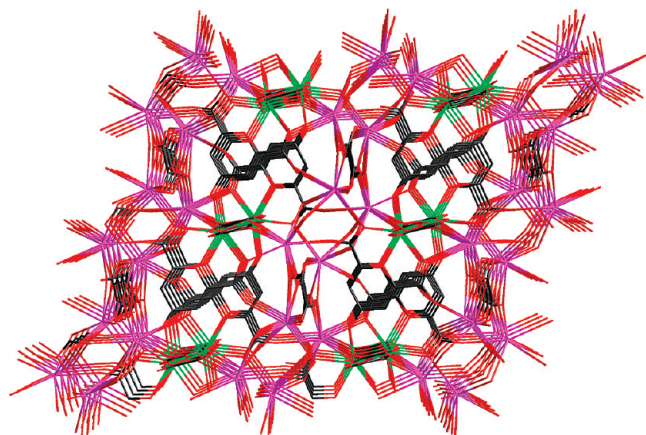


Figure 14. The 3D structure of compound **6**.

both the ligand and oxalate ions are 2-connected, so they can be simplified as a line in the discussion of the topological structure (Figure 13a). Ba^{2+} are also bridged into a 1D chain, then further connected into a 2D layer through oxalate groups. In this layer, the oxalate ion is 4-connected (Figure 13b) and the bridging oxygen can be simplified as a line. The two kinds of layers are further connected into a 3D structure by the CDA ligand (Figure 14).

Crystal Structure of $[\text{Dy}(\text{HCAM})_2(\text{CAM})\text{Ba}_2(\text{H}_2\text{O})_{9.75}] \cdot 7.625\text{H}_2\text{O}$ (7) (CAM = 4-hydroxy-pyridine-2,6-dicarboxylate). Single-crystal X-ray diffraction analyses of **7** exhibits a 1D chain, containing nine-coordinated Dy^{3+} , as well as nine-coordinated (Ba1) and eight-coordinated (Ba2) Ba^{2+} . The crystal was crystallized in the triclinic crystal system, space group $P\bar{1}$. The Dy^{3+} is coordinated by three tridentate(ONO) CAM anions; thus three N atoms and six O atoms complete the coordination sphere of the Dy^{3+} center which displays a tricapped trigonal prism, as shown in Figure 15. The $\text{Dy}-\text{O}$ distances are in the range of 2.400(6)–2.436(6) Å, the $\text{Dy}-\text{N}$ distances are in the range of 2.407(7)–2.463(7) Å. Two carboxylic oxygen atoms and seven water molecules complete the coordination environment of Ba1, and the coordination geometry of Ba1 can be described as a distorted

tricapped trigonal prism. Ba2 center bonds to two carboxylic oxygen atoms and six water molecules, possessing a bicapped trigonal prism geometry, of which O18 is disordered with the position occupancy of 0.7. The $\text{Ba}-\text{O}(\text{carboxylic})$ distances are in the range of 2.657(6)–2.714(7) Å, the $\text{Ba}-\text{O}(\text{aqua})$ distances are in the range of 2.726(16)–2.990(7) Å. Four water molecules acts as bridges between adjacent Ba1 ions to form a binuclear unit-A, and two Ba2 ions construct a binuclear unit-B through two water molecules bridges. Thus the unit-A and -B arrange alternately through the linking of the $[\text{Dy}(\text{CAM})_3]^{3+}$ unit to give rise to a 1D chain, as shown in Figure 16.

Crystal Structure of $[\text{Sm}(\text{CAM})_4\text{Ba}_3(\text{H}_2\text{O})_2]$ (8). The molecule structure of compound **8** with the labeling scheme is shown in Figure 17. The asymmetric unit contains two crystallographically independent Sm^{3+} , three Ba^{2+} , four CAM ligands, and two coordinated water molecules. The two lanthanide ions, Sm1 and Sm2, have a similar coordination environment. They all coordinate with two tridentate (ONO) CAM anions and two hydroxyl oxygen atoms, staying in a distorted bicapped trigonal prism environment, in which the two nitrogen atoms act as the two capping atoms. The $\text{Sm}-\text{O}(\text{carboxylic})$ distances are in the range of 2.400(4)–2.702(4) Å; $\text{Sm}-\text{O}(\text{hydroxyl})$ distances are in the range of 2.353(4)–2.423(4) Å; $\text{Sm}-\text{N}$ distances are in the range of 2.484(5)–2.515(5) Å. There are three types of barium atoms: Ba1, Ba2, and Ba3. Ba1 and Ba2 are nine-coordinated and Ba3 is seven-coordinated. Five carboxylic oxygen atoms, one hydroxyl oxygen atom, and three water molecules construct the coordination sphere of Ba1. Eight carboxylic oxygen atoms and one water molecule finish the nine-coordinated environment of Ba2. Five carboxylic oxygen atoms and two hydroxyl oxygen atoms form the coordination geometry of Ba3. The $\text{Ba}-\text{O}(\text{carboxyl})$ distances are in the range of 2.558(4)–3.006(4) Å, and the $\text{Ba}-\text{O}(\text{aqua})$ ones are in the range of 2.695(4)–3.091(4) Å.

Sm1 and Sm2 are connected into a 1D chain through the CAM ligand, separately, the Sm1-chain and Sm2-chain. The two types of chains arrange alternately and construct a 2D-layer structure by the connection of CAM ligand in the (010) plane. Each CAM coordinates to two Sm^{3+} through tridentate

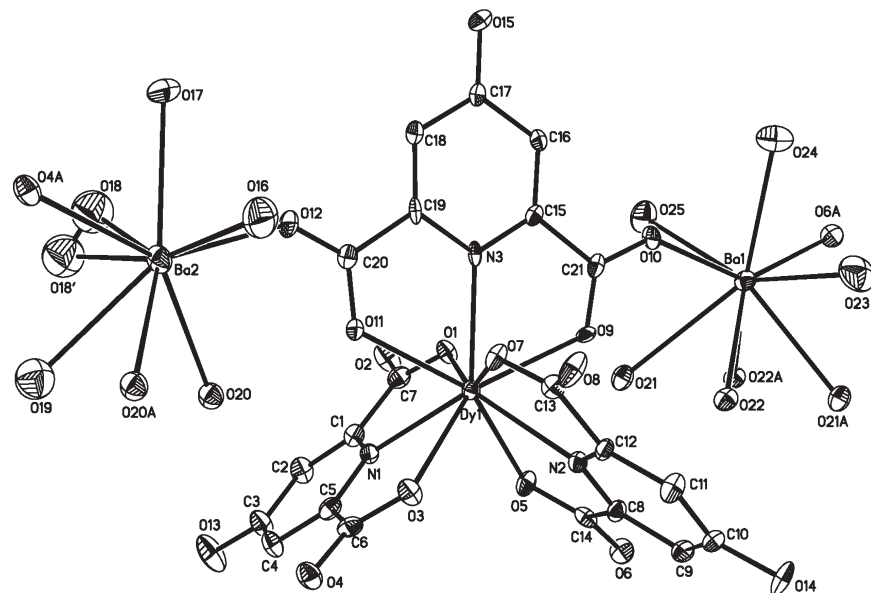
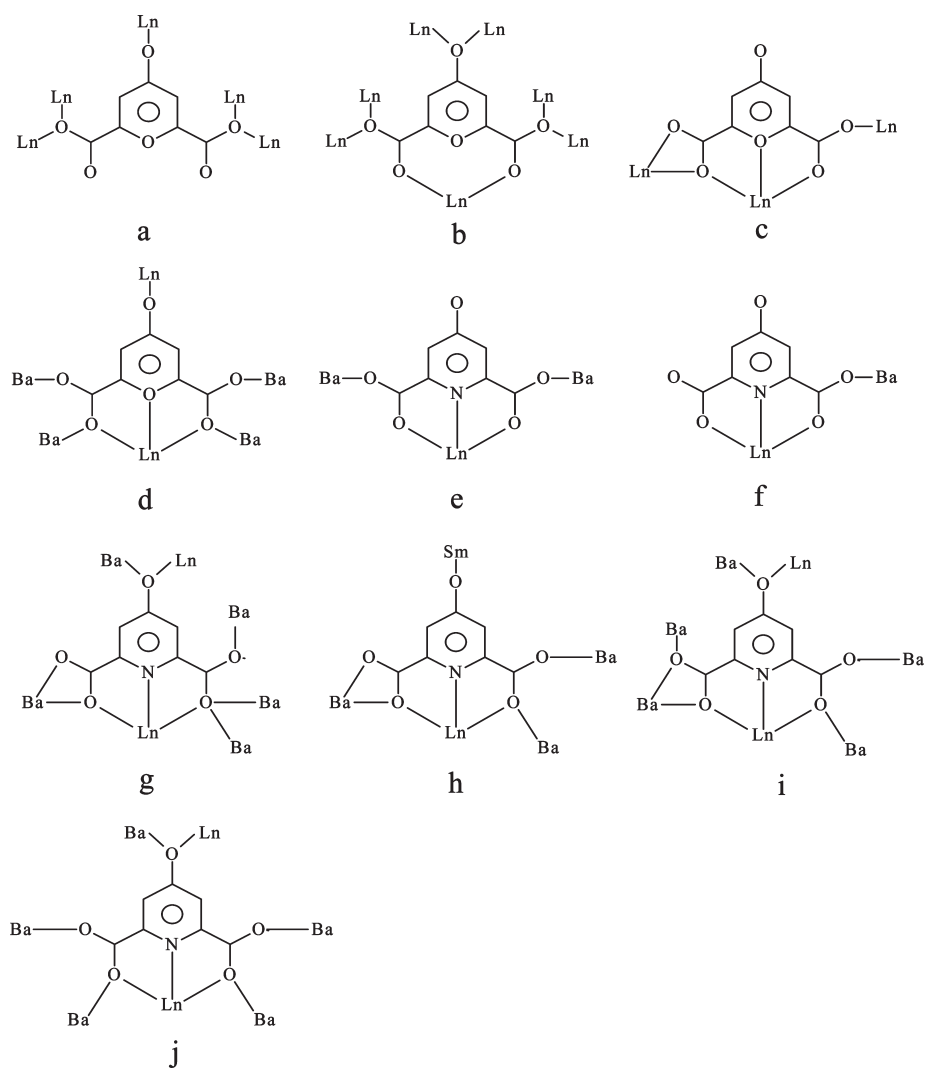


Figure 15. Molecule structure of compound 7.

Chart 1. Coordination Modes in Compounds 1–8



-ONO- and hydroxyl oxygen atom, separately; thus the 2-connected CAM ligand may be simplified as a line in the

discussion of the topological structure in the layer, as shown in Figure 18. Through the bridging of carboxylic oxygen

atoms and water molecules, the barium ions are connected into a 1D chain along the *c* direction (Figure 19); then the 1D chain is further self-assembled into a 2D-layer on the *ac* plane (Figure 20). Topologically, four Ba^{2+} bridged by carboxylic oxygen atoms, forming a tetranuclear unit, is defined as a 8-connected node and the binuclear Ba^{2+} unit is defined as a 6-connected node. Similarly, the ligand can act as a 3-connected node. Consequently, the 2D-layer of Ba^{2+} can be described as a $(3^44^{10}5^46^87^2)(3^44^45^46^3)(3^24)$ topological network. Furthermore, the two kinds of planes arrange alternately, forming a 3D sandwich structure (Figure 21).

Comparison of Structures. In the construction of compounds **1–4**, the lanthanide contraction effect has a great influence on the structure. Compounds **1–3** feature novel 3D frameworks, and **4** is a 2D double-layer structure, although all of them belong to the orthorhombic crystal system with space group *Pnma*. In compound **1**, Pr^{3+} is eight-coordinated, and the average bond length is 2.775 Å. Comparably, Ho^{3+} is six-coordinated, and the average bond length is

2.757 Å in **4**. The decrease of coordination number and average bond length indicates the existence of a lanthanide contraction effect. Compared **5** with **1**, it is important to note that the reaction temperature has a great effect on the structure. When the temperature was changed from 120 to 140 °C, the ligand partly decomposed into oxalate ions, which made the structure of **5** quite different from that of **1**, and the coordination modes have also changed obviously. **1** belongs to orthorhombic crystal system, space group *Pnma*, while **5** belongs to the monoclinic crystal system, space group *C2/c*. The coordination number of Pr^{3+} in compound **1** is eight, and the Pr^{3+} is located in the distorted bicapped trigonal prism. While the coordination number in compound **5** is 10, and the Pr^{3+} is located in a complicated polyhedron. In compound **1**, the ligand act as a heptadentate ligand linking six Pr^{3+} , and the ligand in **5** act as a hexadentate ligand linking three Pr^{3+} .

When LiOH is changed to $\text{Ba}(\text{OH})_2$, heterometal–organic frameworks **6** were obtained. In the reaction, the ligand partly decomposed into oxalate too. For **7** and **8**, the former is a 1D chain and the latter displays a sandwich-like 3D framework, mainly resulting from the lanthanide contraction effect.

Coordination Modes. Compounds **1–6** with four different types of structures, from a 2D double-layer structure, a novel 3D framework, to a 3D heterometallic MOF, display four kinds of coordination modes of CDA anions (Chart 1). In compounds **1–3**, the CDA coordinates to lanthanide ions in mode **b** as a heptadentate ligand. Compound **4** with a 2D

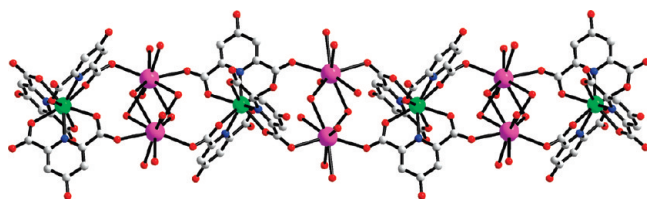


Figure 16. The 1D chain structure of compound **7**. Color codes: red, O; gray, C; blue, N; green, Dy; purple, Ba.

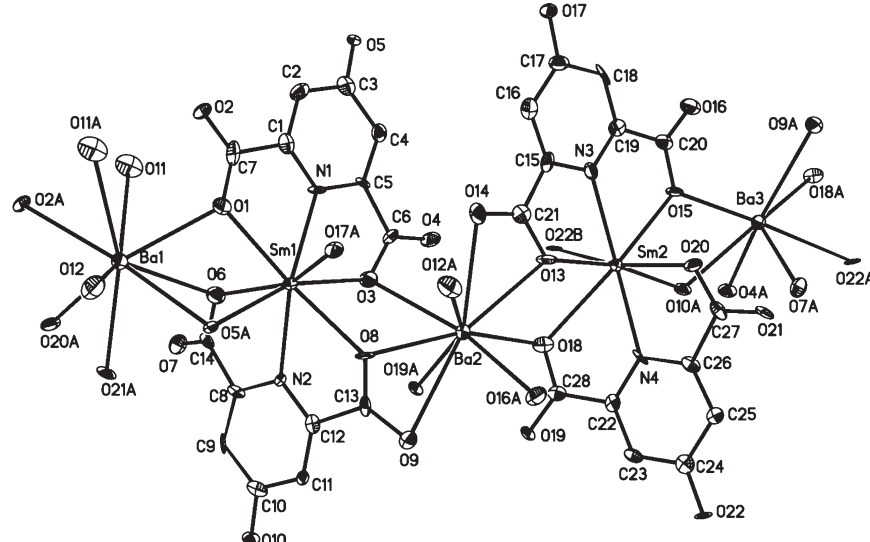


Figure 17. Molecule structure of compound **8**.

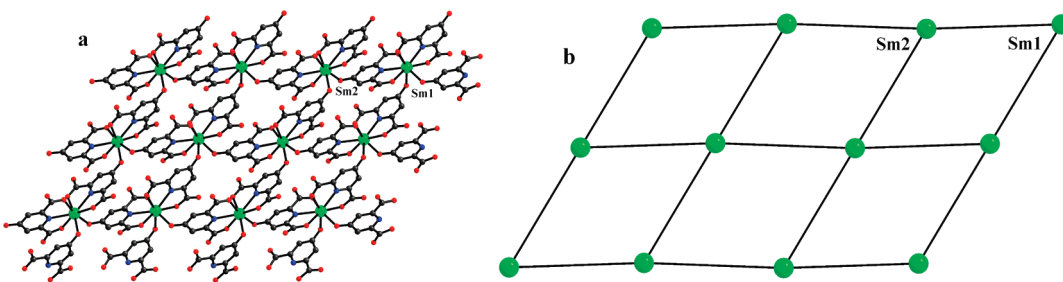


Figure 18. (a) The structure of Sm1-chain and Sm2-chain arranged alternately on the (010) plane of compound **8**. Color codes: red, O; black, C; green, Sm; (b) the topological structure of the 2D layer of Sm^{3+} of compound **8** viewed from the *b* direction.

double-layer structure comprises mode **a**. In compound **5**, mode **c** is observed. In compound **6**, the CDA ligands adopt mode **d** to construct the 3D framework. Compounds **7** with a 1D chain structure and compound **8** with a 3D framework contain six kinds of coordination modes of CAM anions from **e** to **j** (Chart 1). Two types of coordination modes **e** and **f** exist in compound **7**: the CAM anions with coordination mode **e** chelate to one Dy³⁺ and connect two Ba (Ba1 and Ba2) centers. While in mode **f**, each CAM only bonds to one Ba center. Compound **8** possesses four types of coordination modes **g**, **h**, **i**, and **j**: the CAM anion coordinates to Sm1 in modes **i** and **j**, while one coordinates to Sm2 by applying modes **g** and **h**. The differences of coordination modes have a great influence on the assembly of the structure.

Decomposition of H₃CDA. Notably, in compounds **5** and **6**, the CDA ligand partly decomposed into oxalate. Although the reaction mechanism still remains unclear, the oxalate may be formed via an *in situ* oxidation–hydrolysis⁸ reaction of H₃CDA. The hydrolysis reaction may occur at the C–O bond, whereas the oxidation reaction may happen at the C=C bond. The high temperature is responsible for the *in situ* oxidation and hydrolysis of H₃CDA to oxalate, which can be confirmed by the syntheses of compounds **1** and **5** under the same experimental conditions except temperature. Furthermore, the lanthanide ions may act as catalysis for the formation of oxalate.⁸

Spectroscopic Properties. UV–visible spectra of **1** and **2** in the solid state at room temperature show the typical f-f transitions of Pr³⁺ and Nd³⁺ ions (Figure 22). The bands at 592, 485, 471, 446 nm for **1** are four main absorption bands of Pr³⁺ and may be assigned to ³H₄ → ¹D₂, ³H₄ → ³P₀, ³H₄ → ³P₁ or ³H₄ → ¹I₆, ³H₄ → ³P₂, respectively (Figure 22a).⁹ The transition of ³H₄ → ³P₂ belonging to the hypersensitive

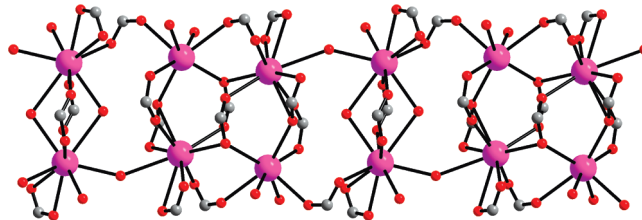


Figure 19. The 1D chain consist of barium ions, carboxylic oxygen atoms and water molecules along *c* direction. Color codes: red, O; gray, C; purple, Ba.

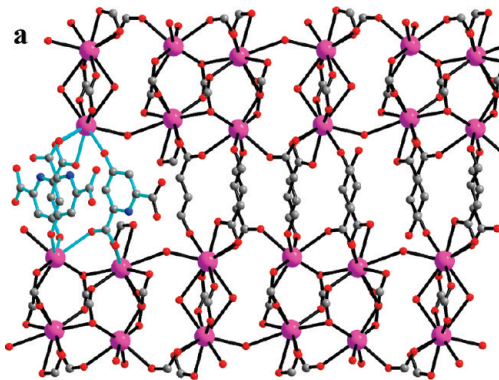


Figure 20. (a) The 1D chain of barium ions was further connected into a 2D-layer on the *ac* plane. (b) The $(3^{44}105^46^87^2)(3^{44}5^46^3)(3^{24})$ topological structure of the 2D layer of Ba²⁺ of compound **8** viewed from the *b* direction. Color codes: red, O; gray, C; blue, N; purple, Ba; blue, the tetranuclear unit; green, binuclear Ba²⁺ unit; yellow, the ligand.

transition corresponds to the band at 445 nm for **1**.¹⁰ Figure 22b displays well-resolved spectral lines of **2**, attributed to Nd³⁺ electronic transitions, from the ⁴I_{9/2} ground state to the following excited levels: ⁴F_{3/2} (867 nm), ⁴F_{5/2} + ²H_{9/2} (798 nm), ⁴S_{3/2} + ⁴F_{7/2} (742 nm), ⁴F_{9/2} (679 nm), ²H_{11/2} (627 nm), ²G_{7/2} + ²G_{5/2} (580 nm), ²K_{13/2} + ⁴G_{7/2} + ⁴G_{9/2} (523 nm), ²K_{15/2} + ²D_{3/2} + ²G_{9/2} (461–475 nm).^{9,11}

Luminescent Properties of Compounds 7 and 8. The solid-state luminescence properties of these compounds were investigated at room temperature. The emission spectrum of compound **7** upon excitation at 280 nm exhibits the two characteristic transition, 474 and 575 nm, which can be assigned to the transitions of ⁴F_{9/2} → ⁶H_{15/2} and ⁴F_{9/2} → ⁶H_{13/2} (Figure 23a),¹² respectively. The three characteristic emission bands in the visible region of compound **8** are depicted in Figure 23b. The three peaks at 564, 604, and 646 correspond to the transitions of Sm³⁺ from ⁴G_{5/2} to ⁶H_J (*J* = 5/2, 7/2, 9/2), respectively.¹³

Magnetic Properties. The magnetic susceptibilities of **5** and **7** were measured in the temperature range from 2 to 300 K and under 1000 Oe field, as shown in Figure 24. The $\chi_M T$ value of **5** and **7** is equal to 1.72, 13.87 cm³ K mol⁻¹ at room temperature, which is close to the theoretical value of 1.60, 14.17 cm³ K mol⁻¹, respectively, expected for one Pr³⁺ in the ³H₄ ground state (*g* = 4/5), or one Dy³⁺ in the ⁶H_{15/2} ground state (*g* = 4/3).¹⁴ For **5** and **7**, the $\chi_M T$ value slowly decreases on cooling and reaches a minimum value of 0.12, 9.65 cm³ K mol⁻¹ at 2 K, respectively.

Theoretically, the lanthanide ions are characterized by the 4fⁿ configuration, which may be split into the ^{2S+1}L_J state due to the interelectronic repulsion and spin–orbit coupling. Influenced by the crystal field perturbation, each of these

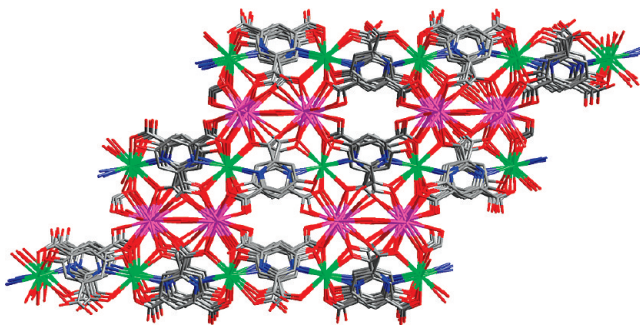


Figure 21. The 3D structure of compound **8**.

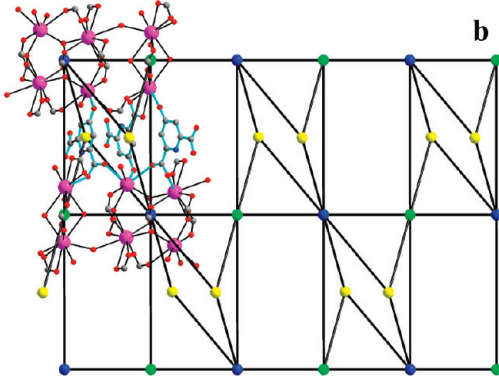


Figure 22. (a) The 1D chain of barium ions was further connected into a 2D-layer on the *ac* plane. (b) The $(3^{44}105^46^87^2)(3^{44}5^46^3)(3^{24})$ topological structure of the 2D layer of Ba²⁺ of compound **8** viewed from the *b* direction. Color codes: red, O; gray, C; blue, N; purple, Ba; blue, the tetranuclear unit; green, binuclear Ba²⁺ unit; yellow, the ligand.

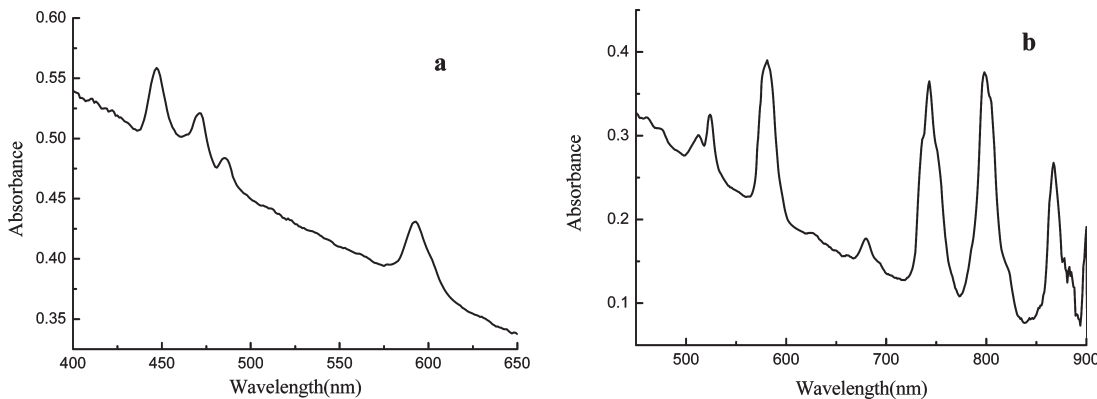


Figure 22. The UV/vis absorption spectra of **1** (**a**) and **2** (**b**) in the solid state.

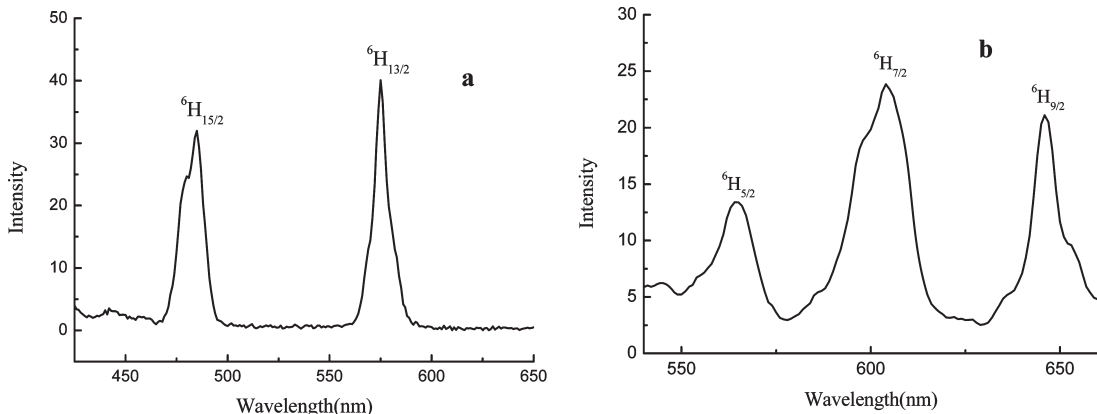


Figure 23. (a) The emission spectra of **7** in solid state when excited at 280 nm; (b) the emission spectra of **8** in the solid state when excited at 280 nm.

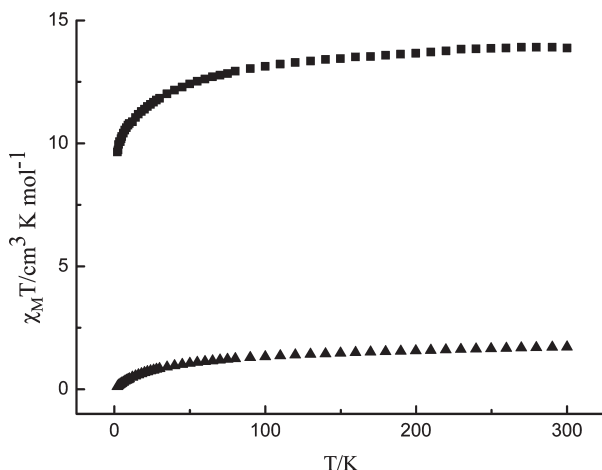


Figure 24. The plots of $\chi_M T$ versus T for, **5** (\blacktriangle) and **7** (\blacksquare).

levels may be further split into Stark sublevels which are thermally populated at room temperature. By lowering the temperature, a depopulation of these sublevels occurs, causing $\chi_M T$ decreases with decreasing temperature. As a result, the nature of the interaction between Ln^{3+} with an orbit angular momentum cannot be inferred clearly when the $\chi_M T$ value decreases with the temperature decrease. Therefore, the nature of the magnetic interaction between Ln^{3+} ions in compounds **5** and **7** cannot be absolutely determined, since the corresponding $\chi_M T$ value of single Ln^{3+} decreases with the temperature decrease.

Conclusion

In summary, eight novel lanthanide-organic frameworks have been constructed by tuning the reaction conditions under hydrothermal syntheses. The structures of **1–4** varied from 3D frameworks to a 2D double-layer, originating from the lanthanide contraction effect. By increasing the reaction temperature from 120 °C for **1** to 140 °C for **5**, compound **5** displays a novel 3D framework different from that of **1**, in which the ligand partly decomposed into oxalate ions. When adjusting the pH value by applying $Ba(OH)_2$, compound **6** was obtained, exhibiting a 3D heterometal-organic framework. Although CDA has a structure similar to CAM, the structures of **7** and **8** were quite different from that of compound **6**. The structural divergence between the 1D chain of **7** and the 3D framework of **8** mainly resulted from the lanthanide contraction effect. The luminescent properties show that complexes **7** and **8** exhibit the characteristic bands of the corresponding lanthanide ions in the solid state. Magnetic investigations reveal that the nature of the magnetic interaction between Ln^{3+} ions in compounds **5** and **7** cannot be absolutely determined due to the disturbance of single Pr^{3+}/Dy^{3+} magnetic behavior.

Acknowledgment. We gratefully acknowledge the NSFC (20501012), FANEDD (200732), NCET-07-0463, NSF of Tianjin (07JCYBJC02000) and 973 Program (2005CB623607).

Supporting Information Available: Crystallographic information files; tables of selected bond lengths and angles in **1–8**; This material is available free of charge via the Internet at <http://pubs.acs.org>.

References

- (1) (a) Pérez-García, L.; Amabilino, D. B. *Chem. Soc. Rev.* **2002**, *31*, 342. (b) Moulton, B.; Zaworotko, M. J. *Chem. Rev.* **2001**, *101*, 1629. (c) Kesani, B.; Lin, W. *Coord. Chem. Rev.* **2003**, *246*, 305. (d) Bradshaw, D.; Claridge, J. B.; Cussen, E. J.; Prior, T. J.; Rosseinsky, M. J. *Acc. Chem. Res.* **2005**, *38*, 273. (e) Zhang, J.; Bu, X. H. *Angew. Chem., Int. Ed.* **2007**, *46*, 6115. (f) Wu, C. D.; Lin, W. B. *Angew. Chem., Int. Ed.* **2007**, *46*, 1075. (g) Liu, Y.; Xu, X.; Zheng, F. K.; Cui, Y. *Angew. Chem., Int. Ed.* **2008**, *47*, 4538. (h) Wu, S. T.; Wu, Y. R.; Kang, Q. Q.; Zhang, H.; Long, L. S.; Zheng, Z. P.; Huang, R. B.; Zheng, L. S. *Angew. Chem., Int. Ed.* **2007**, *46*, 8475. (i) Zhang, J.; Chen, S. M.; Valle, H.; Wong, M.; Austria, C.; Cruz, M.; Bu, X. H. *J. Am. Chem. Soc.* **2007**, *129*, 14168. (j) Lin, Z. J.; Slawin, A. M. Z.; Morris, R. E. *J. Am. Chem. Soc.* **2007**, *129*, 4880.
- (2) (a) Ward, M. D. *Science* **2003**, *300*, 1104. (b) Rosi, N. L.; Eckert, J.; Eddaoudi, M.; Vodak, D. T.; Kim, J.; Keeffe, M. O.; Yaghi, O. M. *Science* **2003**, *300*, 1127. (c) Kitaura, R.; Kitagawa, S.; Kubota, Y.; Kobayashi, T. C.; Kindo, K.; Mita, Y.; Matsuo, A.; Kobayashi, M.; Chang, H. C.; Ozawa, T. C.; Suzuki, M.; Sakata, M.; Takata, M. *Science* **2002**, *298*, 2358. (d) Eddaoudi, M.; Kim, J.; Keeffe, M. O.; Yaghi, O. M. *J. Am. Chem. Soc.* **2002**, *124*, 376. (e) Lin, X.; Jia, J. H.; Zhao, X. H.; Thomas, K. M.; Blake, A. J.; Walker, G. S.; Champness, N. R.; Hubberstey, P.; Schroder, M. *Angew. Chem., Int. Ed.* **2006**, *45*, 7358. (f) Rowsell, J. L. C.; Millward, A. R.; Park, K. S.; Yaghi, O. M. *J. Am. Chem. Soc.* **2004**, *126*, 5666. (g) Surblé, S.; Millange, F.; Serre, C.; Duren, T.; Latroche, M.; Bourrelly, S.; Llewellyn, P. L.; Férey, G. *J. Am. Chem. Soc.* **2006**, *128*, 14889. (h) Rowsell, J. L. C.; Yaghi, O. M. *J. Am. Chem. Soc.* **2006**, *128*, 1304. (i) Dinc, M.; Han, W. S.; Liu, Y.; Dailly, A.; Brown, C. M.; Long, J. R. *Angew. Chem., Int. Ed.* **2007**, *46*, 1419. (j) Dinc, M.; Dailly, A.; Liu, Y.; Brown, C. M.; Neumann, D. A.; Long, J. R. *J. Am. Chem. Soc.* **2006**, *128*, 16876. (k) Panella, B.; Hones, K.; Muller, U.; Trukhan, N.; Schubert, M.; Putter, H.; Hirscher, M. *Angew. Chem., Int. Ed.* **2008**, *47*, 2138. (l) Morris, W.; Doonan, C. J.; Furukawa, H.; Banerjee, R.; Yaghi, O. M. *J. Am. Chem. Soc.* **2008**, *130*, 12626.
- (3) (a) Alkordi, M. H.; Liu, Y. L.; Larsen, R. W.; Eubank, J. F.; Eddaoudi, M. *J. Am. Chem. Soc.* **2008**, *130*, 12639. (b) Dubbeldam, D.; Galvin, C. J.; Walton, K. S.; Ellis, D. E.; Snurr, R. Q. *J. Am. Chem. Soc.* **2008**, *130*, 10884. (c) Rao, C. N. R.; Natarajan, S.; Vaidhyanathan, R. *Angew. Chem., Int. Ed.* **2004**, *43*, 1466. (d) Bradshaw, D.; Prior, T. J. E.; Cussen, J.; Claridge, J. B.; Rosseinsky, M. J. *J. Am. Chem. Soc.* **2004**, *126*, 6106. (e) Gao, E. Q.; Yue, Y. F.; Bai, S. Q.; He, Z.; Yan, C. H. *J. Am. Chem. Soc.* **2004**, *126*, 1419. (f) Cheng, J. W.; Zhang, J.; Zheng, S. T.; Zhang, M. B.; Yang, G. Y. *Angew. Chem., Int. Ed.* **2006**, *45*, 73. (g) Abrahams, B. F.; Moylan, M.; Orchard, S. D.; Robson, R. *Angew. Chem., Int. Ed.* **2003**, *42*, 1848. (h) Kitagawa, S.; Kitaura, R.; Noro, S. *Angew. Chem., Int. Ed.* **2004**, *43*, 2334. (i) Su, C. Y.; Goforth, A. M.; Smith, M. D.; Pellechia, P. J.; zur Loye, H. C. *J. Am. Chem. Soc.* **2004**, *126*, 3576.
- (4) (a) Perry, J. J.; Kravtsov, V. C.; McManus, G. J.; Zaworotko, M. J. *J. Am. Chem. Soc.* **2007**, *129*, 10076. (b) Wang, X. L.; Qin, C.; Wang, E. B.; Li, Y. G.; Su, Z. M.; Xu, L.; Carlucci, L. *Angew. Chem., Int. Ed.* **2005**, *44*, 5824. (c) Ma, S. Q.; Wang, X. S.; Yuan, D. Q.; Zhou, H. C. *Angew. Chem., Int. Ed.* **2008**, *47*, 4130. (d) Paulovi, J.; Cimpoesu, F.; Ferbinteanu, M.; Hirao, K. *J. Am. Chem. Soc.* **2004**, *126*, 3321. (e) Chandler, B. D.; Cramb, D. T.; Shimizu, G. K. H. *J. Am. Chem. Soc.* **2006**, *128*, 10403. (f) Mori, F.; Nyui, T.; Ishida, T.; Nogami, T.; Choi, K. Y.; Nojiri, H. *J. Am. Chem. Soc.* **2006**, *128*, 1440. (g) Prasad, T. K.; Rajasekharan, M. V.; Costes, J. P. *Angew. Chem., Int. Ed.* **2007**, *46*, 2851. (h) Kong, X. J.; Ren, Y. P.; Chen, W. X.; Long, L. S.; Zheng, Z. P.; Huang, R. B.; Zheng, L. S. *Angew. Chem., Int. Ed.* **2008**, *47*, 2398. (i) Liu, G. Z.; Zheng, S. T.; Yang, G. Y. *Angew. Chem., Int. Ed.* **2007**, *46*, 2827. (j) Zhao, B.; Cheng, P.; Chen, X. Y.; Cheng, C.; Shi, W.; Liao, D. Z.; Yan, S. P.; Jiang, Z. H. *J. Am. Chem. Soc.* **2004**, *126*, 3012. (k) Zhao, B.; Chen, X. Y.; Cheng, P.; Liao, D. Z.; Yan, S. P.; Jiang, Z. H. *J. Am. Chem. Soc.* **2004**, *126*, 15394. (l) Yukawa, Y.; Arom, G.; Igarashi, S.; Ribas, J.; Zvyagin, S. A.; Krzystek, J. *Angew. Chem., Int. Ed.* **2005**, *44*, 1997.
- (5) Eubank, J. F.; Kravtsov, V. C.; Eddaoudi, M. *J. Am. Chem. Soc.* **2007**, *129*, 5820.
- (6) (a) Ghosh, S. K.; Neogi, S.; Sanudo, E. C.; Bharadwaj, P. K. *Inorg. Chim. Acta* **2008**, *361*, 56. (b) Gao, H. L.; Yi, L.; Zhao, B.; Zhao, X. Q.; Cheng, P.; Liao, D. Z.; Yan, S. P. *Inorg. Chem.* **2006**, *45*, 5980. (c) Zhao, B.; Gao, H. L.; Chen, X. Y.; Cheng, P.; Shi, W.; Liao, D. Z.; Yan, S. P.; Jiang, Z. H. *Chem.—Eur. J.* **2006**, *12*, 149. (d) Ghosh, S. K.; Ribas, J.; El Fallah, M. S.; Bharadwaj, P. K. *Inorg. Chem.* **2005**, *44*, 3856. (e) Crans, D. C.; Mahroof-Tahir, M.; Johnson, M. D.; Wilkins, P. C.; Yang, L.; Robbins, K.; Johnson, A.; Alfano, J. A.; Godzala, M. E.; Austin, L. T.; Willsky, G. R. *Inorg. Chim. Acta* **2003**, *356*, 365. (f) Devereux, M.; McCann, M.; Leon, V.; McKee, V.; Ball, R. J. *Polyhedron* **2002**, *21*, 1063.
- (7) (a) Sheldrick, G. M. *SHELXL-97, Program for the Solution of Crystal Structures*; University of Gottingen: Germany, 1997. (b) Sheldrick, G. M. *SHELXL-97, Program for the Refinement of Crystal Structures*; University of Gottingen: Germany, 1997.
- (8) (a) Zhang, X. M. *Coord. Chem. Rev.* **2005**, *249*, 1201. (b) Zhang, X. M.; Wu, H. S.; Chen, X. M. *Eur. J. Inorg. Chem.* **2003**, *42*, 2959. (c) Li, X.; Cao, R.; Sun, D.; Shi, Q.; Bi, W.; Hong, M. *Inorg. Chem. Commun.* **2003**, *6*, 815.
- (9) Carnall, W. T.; Fields, P. R.; Wybourne, B. G. *J. Chem. Phys.* **1965**, *42*, 3797.
- (10) Henrie, D. E.; Crosswhite, H. M. *Appl. Opt.* **1963**, *2*, 675.
- (11) Carnall, W. T.; Fields, P. R.; Rajnak, K. *J. Chem. Phys.* **1968**, *49*, 4424.
- (12) Tedeschi, C.; Azéma, J.; Gornitzka, H.; Tisnès, P.; Picard, C. *Dalton Trans.* **2003**, 1738.
- (13) Wang, H. S.; Zhao, B.; Zhai, B.; Shi, W.; Cheng, P.; Liao, D. Z.; Yan, S. P. *Cryst. Growth Des.* **2007**, *7*, 1851.
- (14) Benelli, C.; Gatteschi, D. *Chem. Rev.* **2002**, *102*, 2369.